Origin of rate bistability in Mn–O/Al_2O_3 catalysts for carbon monoxide oxidation: role of the Jahn–Teller effect

Yu.V. Maksimov [a], M.V. Tsodikov [b], E.A. Trusova [b], I.P. Suzdalev [a] and J.A. Navío [c,*]

[a] *N.N. Semenov Institute of Chemical Physics, Russian Academy of Sciences, 4-a ul. Kosygina, 117977 Moscow, Russia*
[b] *A.V. Topchiev Institute of Petrochemical Synthesis, Russian Academy of Sciences, 29 Leninsky prosp., 117912 Moscow, Russia*
[c] *Instituto de Ciencia de Materiales de Sevilla, Centro Mixto CSIC-Universidad de Sevilla, and Departamento de Química Inorgánica, Universidad de Sevilla, c/Américo Vespucio, s/n, 41092 Sevilla, Spain*
E-mail: navio@cica.es

Received 2 August 2000; accepted 18 December 2000

Peculiarities in catalytic activity in carbon monoxide oxidation as well as some structure, electronic and magnetic properties of the three oxide catalysts, Mn^{3+}–O/Al_2O_3 (1), Mn^{3+}–O–Fe/Al_2O_3 (Mn-substituted spinel, 2) and γ-Fe_2O_3/Al_2O_3 (3), were studied by kinetic measurements and by Mössbauer spectroscopy. The catalysts 1 and 2 showed a kinetic bistability with a sharp transition towards more reactive state at ~200 °C (ignition point). In contrast, for catalyst 3, at 200–250 °C, the behavior of reaction rate against temperature did not display noticeable hysteresis. On cooling the catalysts 1 and 2, extinction was observed at about 170 and 120 °C, respectively, i.e., at 30–80 °C lower than the corresponding ignition points. Proximity of activation energy for the high and low activity (~15–19 kJ/mol) for both Mn-containing catalysts suggests an increase in the number of active sites at high temperature with no changes in the reaction mechanism. The considerable difference between Mn-containing catalysts 1, 2 and Fe-containing catalyst 3 may be caused by Jahn–Teller (JT) type distortions of the oxygen polyhedron around Mn^{3+}. A significant spontaneous axial bond stretching within the local polyhedron seems to diminish Mn–O binding energy, facilitate the participation of surface oxygen species, O_S, in the oxidation of CO by a redox mechanism and promote oxygen vacancies at the surface that would cause considerable effect on the activity. An increase in the width of the counterclockwise hysteresis loop for the catalyst 2 compared to the catalyst 1 indicates that clusters of mixed spinel provide more active sites and more labile O_S species than clusters of the binary Mn oxide.

KEY WORDS: CO oxidation; Mn-substituted spinel; clusters of γ-ferric oxide; rate bistability (multiplicity); octahedral complexes of Mn^{3+} (d^4); the Jahn–Teller effect; labile O_S species; anion vacancies; Mössbauer spectroscopy

1. Introduction

The developments concerning new effective exhaust catalysts are related to an increase of the λ-window in three-way catalysts, to a considerable reduction of the noble metal content in catalysts converting NO and NO_2, and to a search for new effective systems for removal of hydrocarbons (HC) and carbon monoxide (CO). Among a number of temperature-resistant catalysts for CO oxidation, the complex oxides are of considerable interest [1–3]. Among the various redox catalytic processes promoted by these systems, the oxidation of CO and the reduction of NO seem to be interesting in view of their relevance for auto-exhaust emission control. A number of correlations of catalytic activity with a variety of physical–chemical properties of perovskites ABO_3 have been discussed in [4]. These correlations are related to the electronic configuration of the B site ion and the B–O bond strength. In a series of perovskites, the complex oxide $LaMnO_3$ exhibits multiple steady states which made possible to suggest two different oxygen states: a chemisorbed atomic species and a more strongly bound oxygen related to the lattice oxygen [5]. For supported complex metal oxides and, in particular, for supported Mn-containing catalysts, the structural and electronic data illuminating the origin of rate multiplicities are still lacking in literature.

The present work deals with the peculiarities of CO oxidation over alumina-supported, manganese-containing catalysts showing rate instability. The origin of this effect is discussed in terms of influence of spontaneous deformation of Mn^{3+} environments caused by the Jahn–Teller effect. Special attention is focused on the formation and participation of surface oxygen species, O_S, and anion vacancies in the reaction mechanism. The electronic and magnetic properties of the iron-containing catalysts are studied by Mössbauer spectroscopy.

2. Experimental

2.1. Catalyst preparation and characterization

The catalysts were prepared by exchange reactions between organometallic compounds: aluminium isopropylate $Al(O^iProp)_3$, ferric acetylacetonate $Fe(acac)_3$ and manganese stearate $Mn(C_{18}H_{35}O_2)_2$. The ligand exchange reactions were carried out in benzene solution with small amount of acetylacetone followed by product condensation. The manganese stearate was preliminary dissolved in a mixture of acetic acid and acetylacetone taken in the ratio 1 : 4.

* To whom correspondence should be addressed.

1011-372X/01/0300-0011$19.50/0

The obtained sols were boiled for 3 h, diluted in ethanol–water solution and repeatedly boiled for 3 h. The obtained gels were dried in air (80 °C, 5 h), under vacuum (80 °C, 10^{-3} Torr, 3 h) and calcined at 500 °C for 6–8 h in air. Elemental analysis of the binary Mn–O/Al_2O_3 (1) and Fe–O/Al_2O_3 (3), and ternary Mn–O–Fe/Al_2O_3 (2) catalysts performed on a Perkin–Elmer AS-400 spectrometer showed the following mass composition: Mn 15, Al 45 and O 40% (1), Fe 14, Mn 2, Al 45 and O 39% (2) and Fe 14, Al 46 and O 40% (3).

The room-temperature Mössbauer spectra were recorded on a conventional gamma-resonance spectrometer operating in a constant-acceleration mode with ^{57}Co(Cr) as source. Isomer shifts (IS) were reported relative to α-Fe. The spectra were computer-analyzed using the common fit procedure for a series of Lorentzians. Phase analysis was performed on a Philips PW 1700 or DRON-3M X-ray powder diffractometer with filtered Cu K_α or Fe K_α irradiation.

2.2. Reaction rate measurements

The reaction of CO oxidation was carried out in the temperature range of 120–500 °C and atmospheric pressure using a plug-flow bed U-shaped quartz reactor. The reactor was placed in a vertical resistively heated thermoprogrammable oven which made possible to maintain the temperature of the catalyst with an accuracy not less than ±1 °C. The standard loading with the powdered catalyst was ∼0.5 cm^3. The ratio $CO/O_2/N_2$ was 1/1/4. Each catalyst was treated with helium with flow rate of 0.06 l/min at 300 °C for 2.5 h before the reaction. All gases used were purified with molecular sieve traps prior to admission into the reactor. A flow rate of reagent mixture was between 60 and 100 standard cm^3/min, which corresponds to an hourly space velocity of 7200–12000. The analysis of reactor effluent was carried out by *in situ* infrared (IR) spectroscopy (Riken Fine RI-500A unit) and by chromatography (Biochrom-1 device, 1.5 m × 3 mm stainless steel column loaded with Inerton RAW + 20% CaA). The catalytic experiments were performed as follows: raising-up the temperature with the rate of 5–10°/min until the necessary temperature was achieved, and passing the reagents through the catalyst until constant activity was reached.

3. Results and discussion

Figure 1 presents the overall CO conversion versus temperature plot for the catalysts 1–3. At the temperatures of 120–200 °C, the catalysts 1 and 2 show negligible activity growth with apparent activation energy of about 19 kJ/mol (figure 1, plots (1) and (2)). However, at $T > 200$ °C, both Mn-containing catalysts exhibit an ignition accompanied by a transient rise in the temperature of the catalyst bed. At $T > 240$ °C, an overall CO conversion reaches ∼95–100% showing, on the Arrenius plot (not presented), an apparent activation energy ∼15–19 kJ/mol. On cooling the catalysts

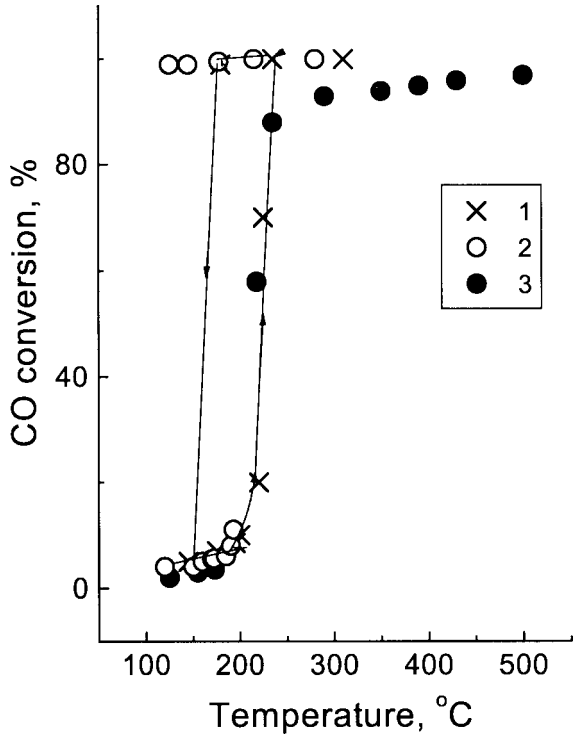

Figure 1. Plots of overall CO conversion versus temperature for the catalysts 1 (Mn–O/Al_2O_3), 2 (Mn–O–Fe/Al_2O_3) and 3 (Fe–O/Al_2O_3).

2 and 3, an extinction is observed at temperatures of about 170 and 120 °C, respectively, about 30–80 °C lower than the ignition temperature. Thus, for both Mn-containing catalysts the counterclockwise hysteresis is typical. Figure 1 shows, as an example, the hysteresis loop for the binary catalyst 1. The difference between the two Mn-containing samples consists in the width of the hysteresis loop: for the ternary catalyst 2, it is wider than for the binary catalyst 1. Thus, at 170–200 °C (catalyst 1) and 120–200 °C (catalyst 2), the two manganese-containing samples exist in two different forms, one which is highly active for CO oxidation, and the other with a lower activity. By keeping the catalysts 1 and 2 at a fixed temperature either in the low or the high activity range, constant conversion is observed for many hours, confirming that the states of both catalysts are truly stable. It should be noted that, in agreement with [5], for supported Mn-containing complex oxides, the hysteresis behavior but not self-organizing oscillations was obtained. The studied catalysts seem also not to be able to spontaneously organize themselves spatially and temporally to start oscillating.

At the temperature range of 120–180 °C, catalyst 3 also implies negligible activity growth with apparent activation energy of about 19 kJ/mol (figure 1, plot 3). However, contrary to catalysts 1 and 2, within the temperature range 180–250 °C, catalyst 3 does not show such a sharp activity growth as catalysts 1 and 2 do. Moreover, for catalyst 3, in the temperature range 250–500 °C, the conversion gradually increases up to ∼90% and does not reach 100% (as it is occurred for catalysts 1 and 2). The value of apparent activation energy for catalyst 3 is a little higher than that of

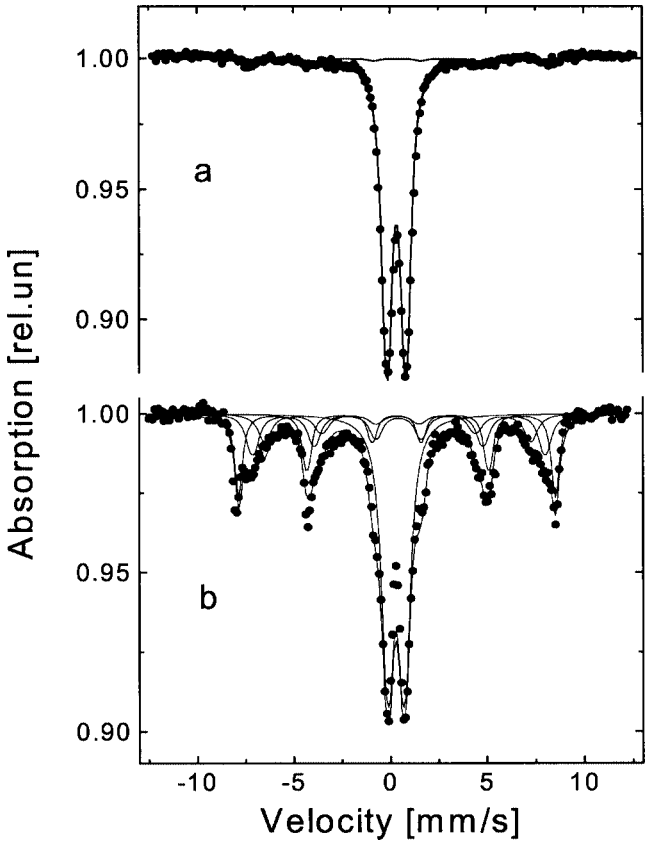

Figure 2. Room-temperature Mössbauer spectra of active catalysts 3 (Fe–O/Al_2O_3) (a) and 2 (Mn–O–Fe/Al_2O_3) (b).

catalysts 1 and 2 (∼25 kJ/mol). At last, again contrary to catalysts 1 and 2, at 180–250 °C, the behavior of reaction rate against temperature does not show noticeable hysteresis, i.e., the plots in figures 1 and 2 are practically the same when measured at rising or falling temperature.

The above data show the strong influence of manganese on the catalytic ability of the supported mixed metal oxides. The similarity in the nature of active sites present on the supported mixed metal oxides 1 and 2 and on $LaMnO_3$ [5] is also quite obvious. The analogy became more apparent when in the present work the flow rate of the reagent mixture was increased by a factor of ten (from an hourly space velocity of about 7200–72000). Despite this increase, the steady-state multiplicities remained invariable indicating that the high efficiency of active sites is not influenced by the extent of surface covering.

The X-ray patterns of the initial catalysts 1–3 show mostly amorphous halo describing poor crystallized structure of γ-Al_2O_3. The Mn-containing catalysts 1 and 2 show broadened reflexes from the doped γ-alumina together with broadened patterns from poorly crystallized Mn_2O_3 (or Mn_3O_4) and Mn-containing spinel with interplanar distances d/n (Å) = 2.70, 2.21, 2.20, 1.84 and d/n (Å) = 2.96, 2.51, 2.08, respectively. The Fe-containing active catalyst 3 is X-ray amorphous.

The ^{57}Fe Mössbauer spectrum for the binary catalyst 3 was fitted to one doublet describing "paramagnetic" high-spin Fe^{3+} sites in the octahedral surroundings of O^{2-} ions in the iron-substituted spinel $Fe_xAl_{2-x}O_3$ [6,7], and to one six-line magnetic pattern with $H_{in} \approx 47.0$ T arising from superparamagnetic clusters of γ-Fe_2O_3 (figure 2(a), table 1). The large value of quadrupole splitting for "paramagnetic" Fe^{3+} sites is due to lattice disorder in alumina alternating stackings and significant axial distortion of local polyhedron FeO_6. The spectrum for the ternary catalyst 2 was fitted to one doublet of octahedral high-spin Fe^{3+} sites, which is similar to that in the catalyst 3, and to six-line magnetic patterns 1–3 (figure 1(b)). Pattern 1 with $H_{in} \approx 50.6$ T is derived from the Fe-rich region arising either from A sites of the Mn-containing spinel [8]) or from a hematite-like phase [9]. Patterns 2 and 3, with $H_{in} \approx 47.0$ and 42.6 T, respectively, are most likely derived from the Mn-poor and Mn-rich regions of B sites in the Mn-containing spinel [8]. The differences in parameters between the Mn-poor and Mn-rich B site are due to the replacement of one or more iron ions on the A site by one or more manganese ions. This replacement affects the superexchange interaction A–O–B and hyperfine field distribution [10].

Table 1
MS parameters at 300 K for "paramagnetic" and magnetic spectral components of active catalysts 3 (Fe–O/Al_2O_3) and 2 (Mn–O–Fe/Al_2O_3).

Catalyst	Component	IS (±0.05 mm/s)	QS (±0.05 mm/s)	H_{in} (±5 T)	Area (%)
Fe–O/Al_2O_3					
	"Paramagnetic"	0.35	0.90	–	∼95
	Magnetic	0.34	0.02	∼47.0	∼5
Mn–O–Fe/Al_2O_3					
	"Paramagnetic"	0.29	0.95	–	47
	Magnetic:				
	(1) Fe-rich	0.34	−0.10	50.6	22
	(2) Mn-poor	0.44	0.02	47.0	18
	(3) Mn-rich	0.39	0.02	42.6	13

From the structural results we conclude:

(i) All studied catalysts show phase separation: catalyst 1 contains poorly crystallized clusters of Mn_2O_3 (or Mn_3O_4) supported on doped amorphous γ-alumina; catalyst 2 includes poorly crystallized clusters of $Mn_xFe_{2-x}O_4$ on amorphous γ-$Fe_xAl_{2-x}O_3$; catalyst 3 consists of X-ray amorphous clusters of γ-ferric oxide and amorphous γ-$Fe_xAl_{2-x}O_3$ as a support.

(ii) Catalysts 2 and 3 contain two types of iron atoms: magnetic iron atoms which are involved in the magnetic superexchange within the Mn-substituted spinel or the γ-ferric oxide clusters and "paramagnetic" iron atoms which are, for both catalysts, octahedral Fe^{3+} sites in the γ-alumina matrix.

(iii) The presence of manganese facilitates magnetic phase separation: for catalyst 2, the fraction of iron in magnetic clusters is ten times larger than in catalyst 3.

(iv) For catalyst 3, γ-ferric oxide clusters show superparamagnetic behavior which makes possible a tentative estimation of mean cluster size $\langle d \rangle \approx 3$–5 nm [7].

Before discussing the kinetic and structure data we consider the following fundamental peculiarity of manganese-containing oxides. Because trivalent manganese ($3d^4$) is a pure Jahn–Teller (JT) ion, and its ^5D ground orbital term is split into a lower doublet and upper triplet under the influence of a crystal field of six octahedrally coordinated oxygen anions, the local elastic distortions are especially probable. With an increase in concentration of manganese, a cooperative distortion along one of the directions ⟨001⟩ would distort the local symmetry of the crystal from cubic to tetragonal. The origin of these site strains is deformation of oxygen ligands about Mn sites. Thus, due to their specific electronic configuration, Mn ions exhibit the JT effects, i.e., they lower their energy by a spontaneous deformation of the local oxygen environment. In the case of Mn-substituted spinels, where both sublattices contain a sufficient amount of JT-active ions, the minimization of the elastic energy induces an ordering of the distortions which leads to a macroscopic tetragonal deformation of the structure [11]. From the kinetic and catalytic point of view, an influence of the JT effect seems to be particularly important for the reaction mechanism. Indeed, this effect leads not only to a noticeable crystallographic distortion of the lattice but also to lowering of the energy of the system, causing a significant spontaneous axial bond stretching [12]. The latter results in lowering of the binding energy of the particular Mn–O_S bond which, in turn, favors more reactivity and surface mobility of the labile oxygen O_S species. An interaction of a CO molecule with such Mn–O_S surface group would result in the creation of an anion vacancy, which is in fact the new catalytically active center, formed upon removal of the oxygen from the surface:

$$\text{Me–O}_S + \text{CO} \rightarrow \text{Me–V}_S + \text{CO}_2 \qquad (1)$$

where V_S is an anion vacancy. As the temperature rises, more active sites Me–V_S are created by the removal of easy-bound surface oxygen. Oxygen from the gas phase can cure the defects and form weakly chemisorbed, labile and reactive surface species:

$$\text{Me–V}_S + \text{O}_2 \rightarrow \text{Me–O}_S + \text{O}_S \qquad (2)$$

The low activation energy for both high- and low-temperature steady states indicates that the reaction rate is controlled by surface diffusion. For catalyst 2, an increase in the width of the hysteresis loop, as compared to catalyst 1, indicates that clusters of mixed spinel $Mn_xFe_{2-x}O_4$ provide more active sites and more labile O_S species than clusters of the binary oxide do in catalyst 1. The surface oxygen O_S reacts more readily with carbon monoxide than lattice oxygen O_L does. Indeed, incorporation of the chemisorbed oxygen into the lattice was found to be a rather slow process [5].

An absence of steady state multiplicity on the Fe-containing catalyst 3 may suggest an easy exchange between surface oxygen O_S and less active (or inactive) lattice species O_L:

$$\text{Me–V}_S + \text{O}_L \rightarrow \text{Me–O}_S + \text{V}_L \qquad (3)$$

This exchange process appears to localize at the interface and leads to a lack of bistability. It should be emphasized that the rate of this exchange, i.e., the rate of the volume lattice oxygen diffusion, is less than that of the surface oxygen diffusion. On the other hand, for catalysts 1 and 2, a low value of activation energy for the high and low activity stages (∼15–19 kJ/mol) suggests surface diffusion as a rate-limiting step of the overall reaction mechanism. As it was mentioned above, for catalyst 3, in the high activity state, an estimate for activation energy gives slightly higher value (∼25 kJ/mol). All these considerations allow us to conclude that for catalyst 3 mass transfer limitations are quite probable. That is why catalyst 3 does not show 100% conversion.

The above explanation is in agreement with the mechanism discussed in [5] for $LaMnO_3$ and $La_{1-x}Sr_xMnO_3$ ($x = 0.2$–0.8). The observed bistability on $LaMnO_3$ and the absence of hysteresis on $La_{1-x}Sr_xMnO_3$ was explained by the fact that the substitution of divalent strontium for the trivalent lanthanum introduces a large number of volume defects (anion vacancies) which results in a much higher ionic conductivity and faster exchange between bulk and surface oxygen.

4. Conclusion

Two types of oxygen, highly reactive and mobile surface species (O_S) and less mobile volume species (O_L) are responsible for carbon monoxide oxidation over Mn-containing and Fe-containing catalysts. Active sites are suggested to be a complex of transition metal and anion vacancy. For Mn-containing catalysts, showing rate bistability, an active site, once formed, is stable even below its temperature of formation, i.e., below the ignition temperature. This results in a counterclockwise hysteresis in the conversion versus temperature plot. For the supported spinel clusters $Mn_xFe_{2-x}O_4$, the width of hysteresis loop exceeds that observed for the supported Mn_2O_3. The origin of the rate instability for Mn-containing catalysts may be caused by Jahn–Teller (JT) type distortions of the oxygen polyhedron around Mn^{3+}. A significant spontaneous axial bond stretching within the local polyhedron decreases Mn–O binding energy and facilitates the participation of surface oxygen O_S in the oxidation of CO by a redox mechanism. An increase in the width of the counterclockwise hysteresis loop for the ternary (spinel) Mn–O–Fe/Al_2O_3 catalyst compared to the binary Mn–O/ Al_2O_3 catalyst indicates that clusters of mixed spinel provide more active sites and more labile O_S species than clusters of the binary Mn oxide. Absence of hysteresis over the binary Fe-containing catalyst suggests an easy exchange between surface and volume species, O_S and O_L, respectively. Thus, the present work has emphasized the possible interplay between a JT lattice distortion of the supported Mn-containing catalysts and their catalytic properties in CO oxidation.

Acknowledgement

The authors thank NATO-Grant (Project ref. ENVIR.LG 971292) and the Russian Foundation for Basic Research (Grant 00–03–32267) for supporting this work.

References

[1] J.P.S. Badyal, X. Zhang and R.M. Lambert, Surf. Sci. Lett. 11 (1990) L15.
[2] T. Ito, A. Kawanami, K. Toi, T. Shirakawa and T. Tokuda, J. Phys. Chem. 92 (1988) 3910.
[3] A.B. Anderson, J. Mol. Catal. 54 (1989) 281.
[4] B. Viswanathan, Catal. Rev. Eng. 34 (1992) 337.
[5] G.K. Chuah, S. Jaenicke and J.Y. Lee, Appl. Catal. 72 (1991) 51.
[6] M.V. Tsodikov, V.Ya. Kugel, Yu.V. Maksimov, O.G. Ellert and O.V. Bukhtenko, J. Catal. 148 (1994) 113.
[7] Yu.V. Maksimov, M.V. Tsodikov, O.G. Ellert, O.V. Bukhtenko and V.V. Matveev, J. Catal. 148 (1994) 119.
[8] G.A. Sawatzky, F. Van Der Woude and A.H. Morrish, Phys. Rev. 187 (1969) 747.
[9] C.R. Bluncson, G.K. Thompson and R.J. Evans, Hyperfine Interact. 90 (1994) 353.
[10] J. Owen and D.R. Taylor, Phys. Rev. Lett. 16 (1969) 1164.
[11] R.E. Vandenberghe and E. De Grave, *Mössbauer Spectroscopy Applied to Inorganic Chemistry*, vol. 2, ed. G.J. Long (Plenum Press, New York, 1987) pp. 59–181.
[12] A.B.P. Lever, *Inorganic Electronic Spectroscopy*, 2nd Ed. (Elsevier, Amsterdam, 1986) p. 218.